ISSN 1392–1207. MECHANIKA. 2014 Volume 20(6): 559–565

Classification of vectors forms dedicated to bearings fault detection of electrical machines based on PSO algorithm

Abla Bouguerne*, Abdesselam Lebaroud**
**Laboratory LGEC Constantine, Department of Electrical Engineering, University of Constantine, Algeria, E-mail: bouguerneabla@yahoo.fr*
***Laboratory LGEC Constantine, Department of Electrical Engineering, University of Skikda, Algeria, E-mail: lebaroud@yahoo.fr*

crossref http://dx.doi.org/10.5755/j01.mech.20.6.6738

1. Introduction

The classification problem has been addressed in many contexts and by researchers in many disciplines. This reflects its broad appeal and usefulness as one of the steps in exploratory data analysis [1]. For explicit classification, it is not necessarily desirable to accurately represent the energy distribution of a signal in time and frequency. In fact, such a representation may conflict with the goal of classification, generating a time–frequency representations (TFR) that maximizes the separability of TFRs from different classes. It may be advantageous to design TFRs that specifically highlight differences between classes [2]. Since all TFRs can be derived from the ambiguity plane, no a priori assumption is made about the smoothing required for accurate classification. Thus, the smoothing quadratic TFRs retain only the information that is essential for classification [3, 4].

Technically, a feature represents a distinguishing property, a recognizable measurement, and a functional component obtained from a section of a pattern. Extracted features are meant to minimize the loss of important information embedded in the signal. In addition, they also simplify the amount of resources needed to describe a huge set of data accurately. This is necessary to minimize the complexity of implementation, to reduce the cost of information processing, and to cancel the potential need to compress the information.

At the interface between the rotor and the stator, the ball bearing is also having a relatively rapid aging. Typically this type of fault is diagnosed by the spectrum of measurement acoustic or vibration [5, 6]. For improved and authentic fault diagnosis using vibration analysis techniques it is necessary that the acquired vibration signals is 'clean' enough that small changes in signal attributes due to an impending fault in any component can be detected [7, 8]. To tackle this problem, we have developed a method based on cloud point dispersion parameter. Since, we used the analytical signals normalized by Hilbert transform of healthy and faulty bearing of induction motor, then extracting vectors forms from time–frequency representation dependant class signal (TFRDCS). Fisher contrast is used to design the kernel nonparametric TFRDCS, It is deliberately designed to maximize separability between classes and minimize the intra-class variance. Recently, the optimization of the size of these vectors realized by particle swarm optimisation (PSO).

2. Analytic signals and Hilbert transform

This representation is commonly used in image processing, where the phase of signal contains more relevant information as the module. Therefore on this principle and for the diagnostic necessary of the asynchronous machine [9] used a phase analysis of the spectrum, and concluded that the information by the phase may be relevant indicative a presence of a fault in the time domain, The Hilbert transform is the convolution of the signal with $(1/t)$ and can underline local properties, as follows:

$$H\left[x(t)\right]=\frac{1}{\pi}\int_{-\infty}^{+\infty}\frac{x(t)}{t-\tau}d\tau=\frac{1}{\pi}x(t)\frac{1}{t}, \tag{1}$$

where t is time, $x(t)$ is a signal in the time domain and $H\left[x(t)\right]$ is Hilbert transformed.

From a signal $x(t)$ and its Hilbert transform $H\left[x(t)\right]$ is obtained the amplitude of signal:

$$A\left[x(t)\right]=x(t)+jH\left[x(t)\right]=a(t)\,e^{j\phi(t)}. \tag{2}$$

The amplitude of the analytical representing the instantaneous amplitude of signal (or envelope) of signal when the signal represents the instantaneous phase, which formulas are given their by:

$$a(t)=\sqrt{x^2(t)+H^2\left[x(t)\right]}, \tag{3}$$

$$\phi(t)=arctan\frac{H\left[x(t)\right]}{x(t)}. \tag{4}$$

The use of the Hilbert transform for the phase analysis is applied to the modulus of the spectrum of the Fourier transform of the signal $x(t)$. Indeed, its analytical signal is given by:

$$A\left[x(f)\right]=x(f)+jH\left[x(f)\right]. \tag{5}$$

The phase of the analytic signal can be expressed by:

$$\phi(f)=arctan\frac{H\left[x(f)\right]}{x(f)}. \tag{6}$$

3. Time-frequency analysis

The problem of diagnosis systems is that they use signals either in the time or frequency domain. In our approach, instead of using a time or a frequency approach, it is potentially more informative to use both time and frequency. Time-frequency analysis of the motor current makes signal properties, related to fault detection, more evident in the transform domain [10].

It is now well accepted that the representations of a signal jointly in time and frequency offer a real interest: they provide a description of the signals non-stationary, that is to say the analysis of laws frequencies signal behaviour over time. The relation between ambiguity plane and TFR has been recognized for a long time. Any bilinear (Cohen class) TFR can be expressed as the two-dimensional Fourier transform of the product of the ambiguity plane of the signal and a kernel function:

$$TFR_x^{\phi}(t,f) = \int_{-\infty}^{+\infty}\left(\int_{-\infty}^{+\infty}\phi(\xi,\tau)A_x(\xi,\tau)\,e^{j2\pi(t\xi-f\tau)}\,d\xi\right)d\tau\,, \quad (7)$$

where t represent time, f represent frequency, η represents continuous frequency shift, and τ represent continuous time lag.

For a given signal $x(t)$ the ambiguity plane $A_x(\xi,\tau)$ is defined as:

$$\begin{aligned} A_X(\xi,\tau) &= \int_{-\infty}^{+\infty} x\left(t+\frac{\tau}{2}\right)x*\left(t-\frac{\tau}{2}\right)e^{-j2\pi\xi t}dt \\ &= \int_{-\infty}^{+\infty}\int_{-\infty}^{+\infty} w_X(t;f)e^{j2\pi(-t\xi+f\tau)}d\xi d\tau \end{aligned} \quad (8)$$

where $x(t+\tau)$ present the signal at a future time $(t+\tau)$, $x*(t+\tau)$ present the complex conjugate of $(t+\tau)$.

For diagnosis, the optimization procedure of TFR Eq. (7) via parameter kernel is computationally very prohibitive. It would be better to use the optimal TFR that can be classified directly in ambiguity plane.

We propose to design and use the classifier directly in the ambiguity plane of Doppler delay. It is possible to view the class dependent TFR and observe the time–frequency structure being exploited by the classifier:

$$RTF_{DCS}[n,k] = F_{\eta\to n}^{-1}\left\{F_{\tau\to k}\left\{\varphi_{DCS}[\eta,\tau]A[\eta,\tau]\right\}\right\} \quad (9)$$

4. Feature extraction

We transform the Fisher's discriminate ratio (FDR) to ϕ_{opt} kernel in a binary matrix by replacing the maximum N points with 1 and the other points with 0, is shown in Fig. 1.

Features can be extracted directly from $\phi_{opt}[\eta,\tau]\circ A[\eta,\tau]$ where o is an element-by-element matrix product. The kernel has the same dimensions as the ambiguity plane. By multiplying the ϕ_{opt} kernel with a certain signal's ambiguity plane, we will find k feature points for this signal. We put them into a vector in order to create the training feature vector $FV_{train}^{(C)}(k)$ of class C :

$$FV_{train}^{(C)}(k) = \phi_{opt}^{(C)}[\eta,\tau]\circ\bar{A}^{(C)}[n,\tau], \quad (10)$$

where $\phi_{opt}^{(C)}[\eta,\tau]$ is the training optimal kernel, $\bar{A}^{(C)}[\eta,\tau]$ is the mean class of ambiguity plane and:

$$\varphi_{opt}^{(C)}[\eta,\tau]\circ\bar{A}^{(C)} = \begin{cases}\bar{A}^{(C)}[\eta,\tau], & \text{if } \varphi_{opt}^{(C)}[\eta,\tau]=1\\ 0, & \text{if } \varphi_{opt}^{(C)}[\eta,\tau]=0\end{cases}. \quad (11)$$

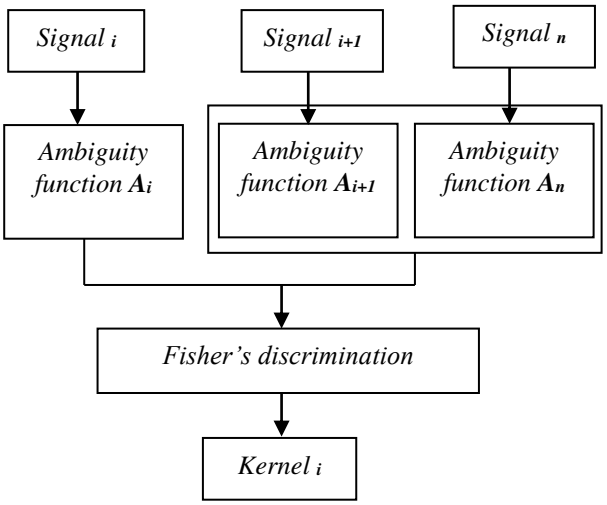

Fig. 1 Kernel design

Feature points are ambiguity plane points of locations (η,τ) where $\phi_{opt}^{(C)}[\eta,\tau]=1$. Selection of points in the Doppler-delay plane is interpreted as masking of the ambiguity function of the signal by an adapted binary function providing an optimal kernel.

5. Particle swarm optimization (PSO)

Particle Swarm Optimization (PSO) was invented by Kennedy and Eberhart1 in the mid 1990s while attempting to simulate the choreographed, graceful motion of swarms of birds as part of a socio-cognitive study investigating the notion of "collective intelligence" in biological populations. In PSO, a set of randomly generated solutions (initial swarm) propagates in the design space towards the optimal solution over a number of iterations (moves) based on large amount of information about the design space that is assimilated and shared by all members of the swarm. PSO is inspired by the ability of flocks of birds, schools of fish, and herds of animals to adapt to their environment, find rich sources of food, and avoid predators by implementing an "information sharing" approaches, hence, developing an evolutionary advantage. References 1 and 2 describe a complete chronicle of the development of the PSO algorithm form merely a motion simulator to a heuristic optimization approach [11, 12].

The basic PSO algorithm consists of three steps, namely, generating particles' positions and velocities, velocity update, and finally, position update. Here, a particle refers to a point in the design space that changes its position from one move (iteration) to another based on velocity updates. First, the positions x_k^i, and velocities v_k^i, of the initial swarm of particles are randomly generated

using upper and lower bounds on the design variables values x_{min} and x_{max}, as expressed in Eqs. (1) and (2). The positions and velocities are given in a vector format with the superscript and subscript denoting the i^{th} particle at time k. In Eqs. (1) and (2), rand is a uniformly distributed random variable that can take any value between 0 and 1. This initialization process allows the swarm particles to be randomly distributed across the design space.

$$x_0^i = x_{min} + rand\left(x_{max} - x_{min}\right) \tag{12}$$

$$v_0^i = \frac{x_{min} + rand\left(x_{max} - x_{min}\right)}{\Delta t} \tag{13}$$

The second step is to update the velocities of all particles at time $k+1$ using the particles objective or fitness values which are functions of the particles current positions in the design space at time k. The fitness function value of a particle determines which particle has the best global value in the current swarm P_k^g, and also determines the best position of each particle over time P^i, i.e. in current and all previous moves. The velocity update formula uses these two pieces of information for each particle in the swarm along with the effect of current motion v_k^i, to provide a search direction v_{k+1}^i, for the next iteration.

The velocity update formula includes some random parameters, represented by the uniformly distributed variables, rand, to ensure good coverage of the design space and avoid entrapment in local optima. The three values that effect the new search direction, namely, current motion, particle own memory, and swarm influence, are incorporated via a summation approach as shown in equation 3 with three weight factors, namely, inertia factor w, self confidence factor c_1, and swarm confidence factor c_2, respectively [13, 14]:

$$v_{k+1}^i = w v_k^i + c_1\, rand \frac{\left(P^i - x_k^i\right)}{\Delta t} + c_2\, rand \frac{\left(P_k^g - x_k^i\right)}{\Delta t}. \tag{14}$$

The original PSO algorithm1 uses the values of *1*, *2* and *2* for w, c_1, and c_2 respectively, and suggests upper and lower bounds on these values as shown in Eq. (3) above. However, the research presented in this paper found out that setting the three weight factors w c_1, and c_2 at 0.5, 1.5, and 1.5 respectively provides the best convergence rate for all test problems considered. Other combinations of values usually lead to much slower convergence or sometimes non-convergence at all.

The tuning of the PSO algorithm weight factors is a topic that warrants proper investigation but is outside the scope of this work. For all the problems investigated in this work, the weight factors use the values of 0.5, 1.5 and 1.5 for w, c_1 and c_2 respectively. The position update is the last step. The Position of each particle is updated using its velocity vector as shown in Eq. (4) and depicted in Fig. 2:

$$x_{k+1}^i = x_k^i + v_{k+1}^i \Delta t\,. \tag{15}$$

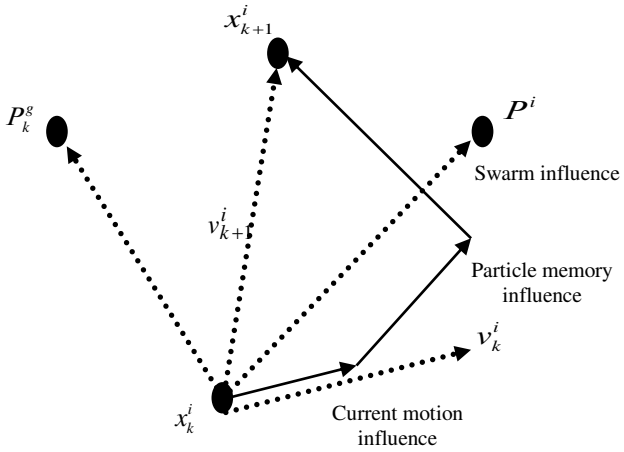

Fig. 2 Depiction of the velocity and position updates in particle swarm optimization

The three steps of velocity update, position update, and fitness calculations are repeated until a desired convergence criterion is met. In the PSO algorithm implemented in this study, the stopping criteria is that the maximum change in best fitness should be smaller than specified tolerance for a specified number of moves, S, as shown in Eq. (16) [12]. In this work, S is specified as ten moves and ε is specified as 10^{-5} for all test problems.

$$\left|f\left(P_k^g\right) - f\left(P_{k-q}^g\right)\right| \le \varepsilon \quad q = 1,2,...,S \tag{16}$$

The main advantages of the PSO algorithm are [13]: simple concept, easy implementation, robustness and computational efficiency compared with the mathematical algorithm and other heuristic optimization techniques. These superior features make PSO a highly viable candidate to be used to solve the multi-objective optimization problems. In this chapter we will use the PSO to optimize the size of the vectors extracted from the forms TFRDCS.

6. Experiment results

6.1. The experimental test bed PRONOSTIA

The proposed method is verified on experimental vibration signals taken from the test bed PRONOSTIA, designed and realized within FEMTO-ST institute [15]. This test bed has been developed to test and validate the fault detection, diagnostic and prognostic algorithms of ball bearings. The aim of the test bed PRONOSTIA is to provide realistic data which characterize the natural degradation of bearings throughout their useful life. This test bed helps to accelerate the aging of bearings by applying severe operating conditions by varying the rotation speed and by applying a radial force greater than that one recommended by the manufacturer. These constraints allow simulating the degradation of ball bearings in few hours.

The test bed is composed of a ball bearing of type NSK 6804RS installed on a shaft, as shown in Fig. 3. The characteristics of this bearing are given in Table.

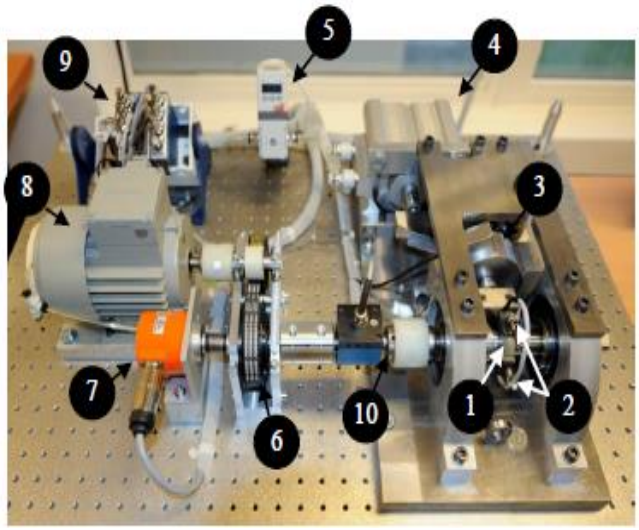

1- Test bearing
2- Accelerometers
3- Force sensor
4- Pneumatic jack
5- Pneumatic regulator
6- Pulleys
7- Speed recorder
8- AC motor
9- Acquisition system
10-Coupling

Fig. 3 The experimental test bed PRONOSTIA [15]

Table
Characteristics of the studied bearing

Diameter of rolling elements, mm	3.5
Number of rolling element	13
Diameter of the outer race, mm	29.1
Diameter of the inner race, mm	22.1
Bearing mean diameter, mm	25.6

Fig. 4 depicts an example of what one can observe on the ball bearing components before and after an experiment, as well as a vibration raw signal gathered during a whole experiment. Note that the degradation of bearings depicts very different behaviors leading to very different experiment duration (until the fault).

Fig. 4 Normal and degraded bearings

6.2. Training set

The vibration signals are composed of 2560 samples recorded every 10 seconds with a sampling frequency equal to 25.6 kHz. We cannot use the vibration signals directly due to their very low values. We have proposed a method for calculating a parameter very interesting, the dispersion parameter of the cloud of points ξ . This parameter is used to calculate the TFR and extraction feature vectors.

6.3. Data treatment by Hilbert transforms

We can easily conclude that the signatures induced in vibration signal analyzed by the Hilbert transform are more pronounced than those induced in the spectrum of signal.

We have proposed a method based a pretreatment Data by Hilbert transform for calculating a very interesting parameter to know the cloud points dispersion parameter ξ :

$$\xi = \sum_{K=1}^{Nva} \left(A_K - \tilde{V}' a_{Re,Im} \right) \left(A_K - \tilde{V}' a_{Re,Im} \right)^T , \qquad (17)$$

where $\tilde{V}' a_{Re}$, $\tilde{V}' a_{Im}$ are coordinates of point A_K .

This parameter ξ is used to calculate the TFR and extraction vectors forms.

As a side from a representation of the cloud points dispersion ξ of Analytics Vibration Signal for a healthy machine and bearing faults (Fig. 5) to remark that the cloud points dispersion ξ for bearing fault are much separated compared with a healthy machine while the points of the same classes are very approximations.

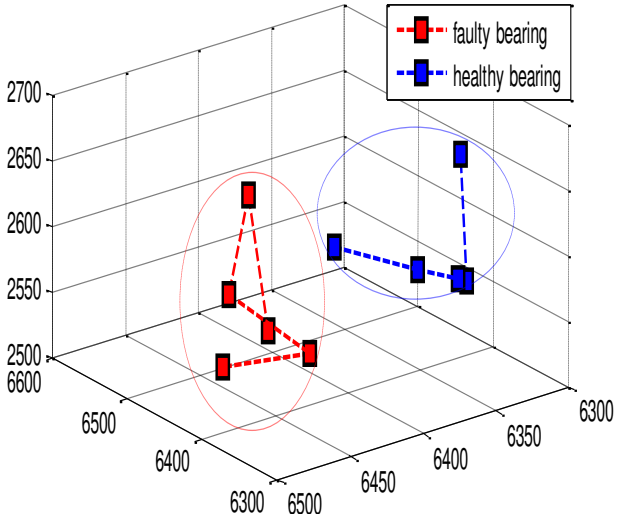

Fig. 5 Representation cloud points dispersion of analytical vibration signals (AVS)

6.4. Vectors forms optimization by PSO

The optimization of analytical vibration signal will be do by PSO method, With the optimization criterion, the optimization of vectors form will be fitting and executing to extract pertinent points. We were able to reduce the size of point in the vector from twenty to ten points. Thus the analytical vibration signal with healthy (Figs. 6 and 7) or bearing failure (Figs. 8 and 9) is characterized by ten points each relevant also called scores or high contrast in the sense of Fisher. These vectors can be easily used by beings classification techniques or artificial intelligence.

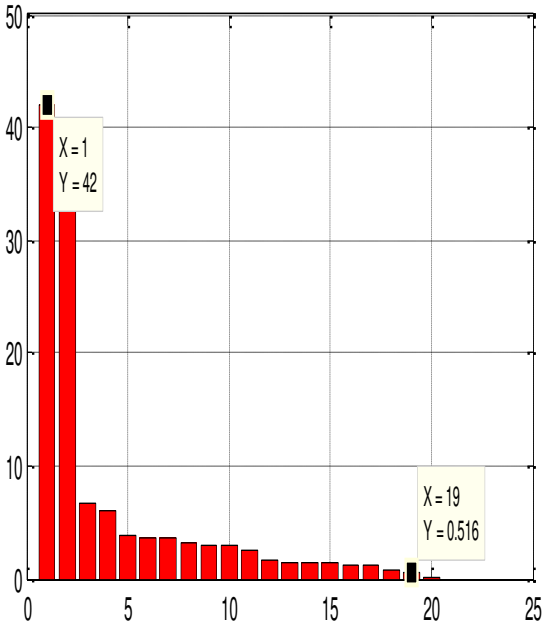

Fig. 6 Vector forms of healthy machine before optimization

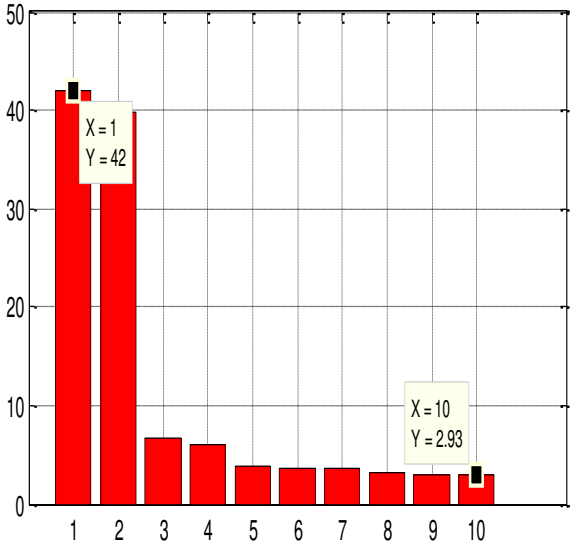

Fig. 7 Vector forms optimize by PSO of healthy machine

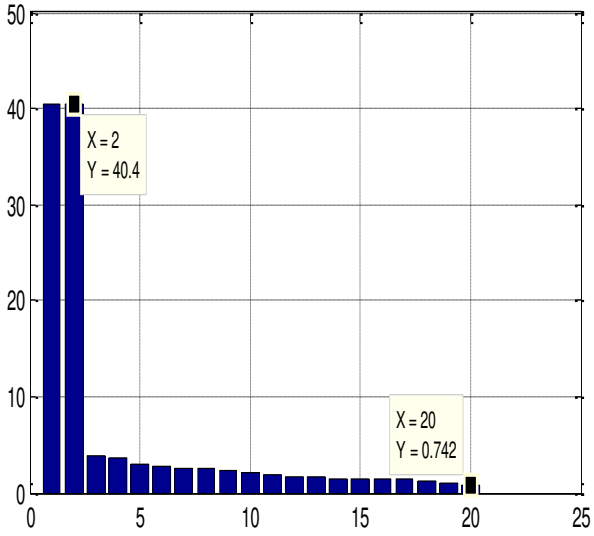

Fig. 8 Vector forms of bearing fault before optimization

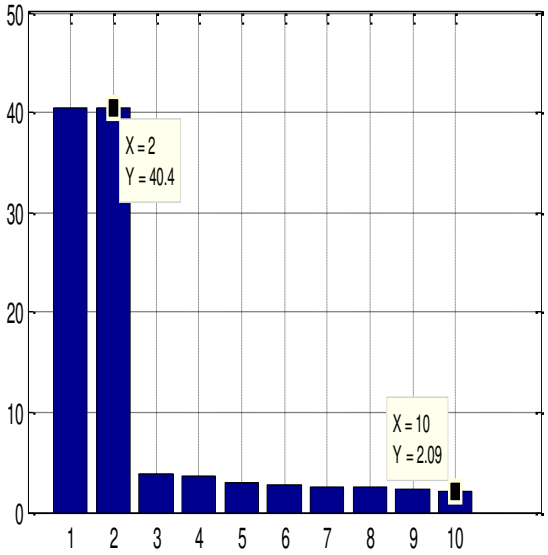

Fig. 9 Vector forms optimize by PSO of bearing fault

Figs. 10 and 11 have respectively a representation of vectors forms before optimization and optimized by PSO. Theses figure Shawn clearly classes position for vector forms of analytical vibration signals. These figures give us a separation between healthy machine and bearing fault class.

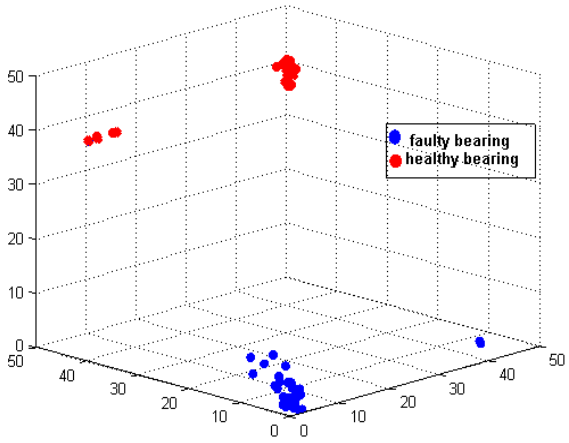

Fig. 10 Classes position for vector forms before optimization

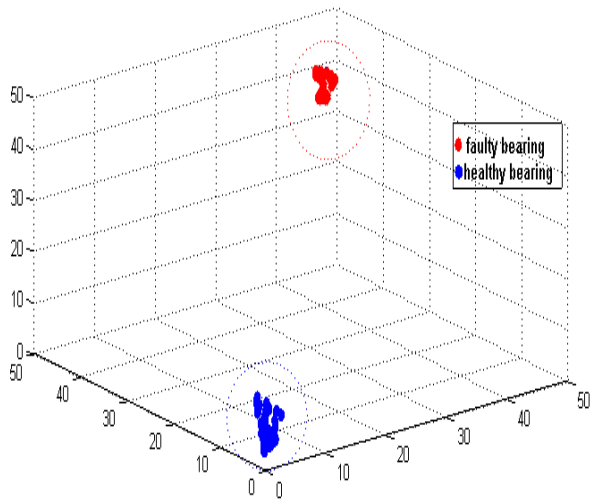

Fig. 11 Classes position for vector forms optimized by PSO

7. Conclusion

In this paper, we have proposed a new method for calculating a very interesting parameter, that dispersion of cloud parameter of points. Since we cannot use the vibration signals directly due to their very low values.. This parameter is used to calculate the TFR and extraction feature vectors.

The simulation results have shown a representation of the dispersion of cloud points of Vibration Analytics Signal (AVS) for a healthy and faulty bearing that the dispersion parameter confirms the separability of classes (healthy bearing class and faulty bearing class). then we made the extraction of the vector formed by the RTF and the separation of classes by filtering (kernel Fischer) and the following we have optimized by PSO; these processing gives us a separation between healthy bearing and faulty. The main advantages of the PSO algorithm are simple concept, easy implementation, robustness and computationnal efficiency compared with the mathematical algorithm and other heuristic optimization techniques. These superior features make PSO a highly viable candidate to be used to solve the multi-objective optimization problems.

References

1. **Ondel, O.; Boutleux, E.; Clerc,G.** 2005. Feature selection by evolutionary computing: Application on diagnosis by pattern recognition approach, In Sergiu Dascalu, ed., CAINE, ISCA: 219-225. http://dblp.uni-trier.de/db/conf/caine/caine2005.html#OndelBC05.
2. **Lebaroud, A.; Clerc, G.** 2008. Classification of induction machine faults by optimal time-frequency representations, IEEE Transactions on Industrial Electronic 55(12): 4290-4298. http://dx.doi.org/10.1109/TIE.2008.2004666.
3. **Wang, M.; Rowe, G. I.;Mamishev A.V.** 2004. Classification of power quality events using optimal time-frequency representations—Part 2: application, Power Delivery, IEEE Transactions 19: 1496-1503. http://dx.doi.org/10.1109/TPWRD.2004.829869.
4. **Soualhi, A.; Clerc, G.; Razik, H.; Ondel, O.** 2011. Detection of induction motor faults by an improved artificial ant clustering, IECON 2011 - 37th Annual Conference on IEEE Industrial Electronics Society: 34463451. http://dx.doi.org/10.1109/IECON.2011.6119866.
5. **Ocak, H.; Loparo, K.A.** 2004. Estimation of the running speed and bearing defect frequencies of an induction motor from vibration data, Mechanical Systems and Signal Processing 18(3): 515-533. http://dx.doi.org/10.1016/s0888-3270(03)00052-9.
6. **Blodt, M.; et al.** 2008. Models for bearing damage detection in induction motors, IEEE transactions on industrial electronics 55(4). http://dx.doi.org/10.1109/TIE.2008.917108.
7. **Zhou, W.; Habetler, T.G.; Harley, R.G**. 2007. Stator current-based bearing fault detection techniques: A general review, IEEE International Symposium on. Diagnostics for Electric Machines, Power Electronics and Drives: 7-10. http://dx.doi.org/10.1109/DEMPED.2007.4393063.
8. **Santhana Raj, A.; Murali, N**. 2013. early classification of bearing faults using morphological operators and Fuzzy inference, IEEE Transactions on Industrial Electronics 60(2): 567-574. http://dx.doi.org/10.1109/TIE.2012.2188259.
9. **Marcelo, C.; Fossatti, J.P; Terra**, **J.I.** 2012. Fault diagnosis of induction motors based on FFT, Signal Processing, Dr Salih Salih (Ed.), ISBN: 978-953-51-0453-7, InTech. http://dx.doi.org/10.5772/37419.
10. **Didier, G.; Ternisien, E.; Caspary, O.; Razik, H.** 2007. A new approach to detect broken rotor bars in induction machines by current spectrum analysis, Mechanical Systems and Signal Processing, Elsevier 21(2): 1127-1142. http://dx.doi.org/10.1016/j.ymssp.2006.03.002**.**
11. **Clerc, M.; Kennedy, J**. 2002. The particle swarm-explosion, stability, and convergence in a multidimensional complex space, Evolutionary Computation, IEEE Transactions 6 (1): 58-73. http://dx.doi.org/10.1109/4235.985692.
12. **del Valle, Y.; et al.** 2008. Particle swarm optimization: basic concepts, variants and applications in power systems, Evolutionary Computation, IEEE Transactions 12(2): 171-195. http://dx.doi.org/10.1109/TEVC.2007.896686.
13. **Abido, A.** 2002. Optimal power flow using particle swarm optimization, Int. J. Elect. Power Energy Syst, 24(7): 563-571. http://dx.doi.org/10.1016/S0142-0615(01)00067-9.
14. **Bergh, F.; Engelbrecht, A**. 2004. A cooperative approach to particle swarm optimization, IEEE Transactions on Evolutionary Computation 8(3): 225-239. http://dx.doi.org/10.1109/TEVC.2004.826069.
15. **Nectoux, P.; Gouriveau, R.; Medjaher, K.; Ramasso, E.; Morello, B.C.; Zerhouni, N.; Varnier, C.** 2012. PRONOSTIA: An Experimental Platform for Bearings Accelerated Life Test. IEEE International Conference on Prognostics and Health Management, PHM'12, Jun2012, Denver, Colorado, United States. IEEE Catalog Number: 1-8. http://www.femto-st.fr/en/Research-departments /AS2M/Research groups /PHM /IEEE -PHM-2012-Data-challenge.php.

A. Bouguerne, A. Lebaroud

ELEKTROS MAŠINŲ GUOLIŲ DIAGNOSTIKOS VEKTORIŲ FORMŲ KLASIFIKAVIMAS DALELIŲ SPIEČIAUS OPTIMIZAVIMO (PSO) ALGORITMO PAGRINDU

R e z i u m ė

Išankstinis guolių defektų išaiškinimas ir diagnozavimas operatyviai užkerta kelią nenormaliam defekto progresavimui ir guolio produktyvumo praradimui. Guolio virpesių signalų analizė dėka savo efektyvumo ir nesudėtingo valdymo yra vienu iš plačiausiai taikomų metodų guolių diagnostikoje. Per paskutinius kelis dešimtmečius guolio laiko-dažnio charakteristikos analizė plačiai taikoma guolių defektų nustatyme. Pagrindiniu šios procedūros veiksniu yra informatyvių savybių išskyrimas iš laiko-

dažnio diagramos. Tyrimo rezultatai remiasi šiam tikslui įgyvendinti išplėtotu dispersinės analizės metodu. Reikiamo požymio išskyrimo esmė yra ta, kad sugedusio mechanizmo laiko-dažnio diagrama analizuojama pagal skirtingas gedimų klases. Individualus laiko-dažnio diagramos sudarytos kiekvienai gedimų klasei. Išskirto požymio vektoriaus dydis yra optimizuotas panaudojant Dalelių Spiečiaus Optimizavimo metodą. Šis priartėjimas yra taikomas bendruoju atveju ir po to patikrinamas PRONOSTIA eksperimentine įranga.

A. Bouguerne, A. Lebaroud

CLASSIFICATION VECTORS FORMS DEDICATED TO BEARINGS FAULT DETECTION OF ELECTRICAL MACHINES BASED ON PSO ALGORITHM

S u m m a r y

Early detecting and diagnosing bearing defects during operation aid in preventing abnormal fault progression and decrease productivity loss. Vibration signal analysis is one of the most widely applied methods for bearing problem diagnosis, for its effectiveness and easy manipulation. Time-frequency analysis has received considerable interest in the field of bearing fault detection over the past few decades. A key element of this procedure is extracting informative features from the TFRs. In this report, we have developed a method based on cloud point dispersion parameter. The essence of the feature extraction is to project from faulty machine to a low size signal time-frequency representation (TFR), which is deliberately designed for maximizing the separability between classes, a distinct TFR is designed for each class. The feature vectors size is optimized using Particle Swarm Optimization method (PSO). This approach is validated on an academic case and then tested on real data taken from the PRONOSTIA experimental platform.

Keywords: Time-frequency representations, analytic vibration signal, dispersion parameter, Hilbert transform particle swarm optimization.

Received February 07, 2014
Accepted December 15, 2014